

# Cyclopropanediamines. 6.<sup>1</sup> Autocatalytic Conversion of 1-Methyl-*r*-1,*t*-2-cyclopropanediamine into 4-Aminobutan-2-one in Aqueous Buffer Solutions of pH 6.5–10. Azomethine Ylides as Intermediates in the Catalysis by Alkyl Ketones<sup>†</sup>

Wolfgang von der Saal<sup>\*,2</sup> and Helmut Quast<sup>\*</sup>

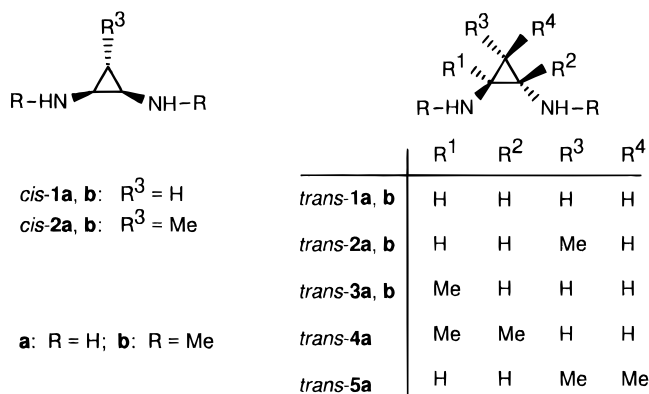
Institut für Organische Chemie der Universität Würzburg, Am Hubland, D-97074 Würzburg

Received December 6, 1995<sup>®</sup>

The  $pK_a$  values of 1,2-cyclopropanediammonium dibromides (**1**–**5**·2HBr) were determined by potentiometric titration with KOH. Corrections for overlapping ionizations and for the varying ionic strength were employed in the calculation of the thermodynamic acidities. The equilibrium constant  $K_E = 2.9$  of the two monoprotonated forms of *trans*-**3b**·H<sup>+</sup> was derived from the  $pK_a$  values and the pH dependence of proton spectra which were interpreted with the help of nuclear Overhauser experiments. The autocatalytic conversion of *trans*-**3a**·2HBr into 4-aminobutan-2-one (**8**) in various buffer solutions of pH = 6.5–10 was monitored by proton spectroscopy. This sequence of reactions is subject to a general acid/base catalysis and also catalyzed by acetone and butanone.

## Introduction

Recently, we have shown that the 1,2-cyclopropanediammonium dibromides, **1**·2HBr to **5**·2HBr, are stable in aqueous mineral acids. In phosphate buffer solutions of pH = 5.8 at 25 °C, however, **1**–**4** begin to decompose after an initiation period of several hours, while **5** is stable under these conditions.<sup>3</sup> The products are unstable as well, with the exception of 4-aminobutan-2-one (**8**), which arises almost quantitatively from *trans*-**3a**·2HBr. In order to provide a background for a detailed mechanistic picture of these reactions, we now report the macroscopic thermodynamic acidity constants of **1**·2HBr to **5**·2HBr and the equilibrium constant of the two monoprotonated forms of *trans*-**3b**·H<sup>+</sup>. Subsequently, we detail the kinetics of the conversion of *trans*-**3a**·2HBr into **8** and describe the influence of various buffer solutions and ketones on the rate constants of this autocatalytic reaction.



## Methods and Results

### $pK_a$ Values of 1,2-Cyclopropanediammonium Ions.

The macroscopic acidity constants  $K_1$  and  $K_2$  at 25 °C

**Table 1.** Thermodynamic Acidity Constants of the 1,2-Cyclopropanediammonium Dibromides **1**·2HBr to **5**·2HBr and of Some Model Compounds in Water at 25 °C

compound	$pK_{a1}$	$pK_{a2}$
<i>cis</i> - <b>1a</b> ·2HBr	4.20	9.04
<i>trans</i> - <b>1a</b> ·2HBr	5.90	8.82
<i>cis</i> - <b>1b</b> ·2HBr	3.56	8.73
<i>trans</i> - <b>1b</b> ·2HBr	5.65	8.73
<i>cis</i> - <b>2a</b> ·2HBr	4.35	8.98
<i>trans</i> - <b>2a</b> ·2HBr	5.90	8.98
<i>cis</i> - <b>2b</b> ·2HBr	3.68	9.13
<i>trans</i> - <b>2b</b> ·2HBr	5.68	9.03
<i>trans</i> - <b>3a</b> ·2HBr	5.83	9.06
<i>trans</i> - <b>3b</b> ·2HBr	5.52	9.05
<i>trans</i> - <b>4a</b> ·2HBr	5.94	9.03
<i>trans</i> - <b>5a</b> ·2HBr	5.97	8.96
<i>cis</i> -1,2-cyclobutanediamine <sup>5</sup>	5.40	9.22
<i>trans</i> -1,2-cyclobutanediamine <sup>5</sup>	6.66	9.65
<i>cis</i> -1,2-cyclohexanediamine <sup>6</sup>	6.13	9.93
<i>trans</i> -1,2-cyclohexanediamine <sup>6</sup>	6.47	9.94
1,2-ethanediamine <sup>6</sup>	6.85	9.93
<i>N,N</i> -dimethyl-1,2-ethanediamine <sup>6</sup>	7.47	10.29

were determined by potentiometric titration with 0.1 M KOH of 0.05 M solutions of the diammonium dibromides **1**·2HBr to **5**·2HBr in carbon dioxide-free water. Special measures were taken to avoid errors due to *cis*–*trans* isomerization or decomposition during the titration. As mentioned in the Introduction, such reactions are to be expected in neutral solutions. Therefore, we determined  $K_1$  by titrating the first deprotonation step in the range of pH = 3.0–6.5 and subsequently, using a freshly prepared solution,  $K_2$  in the range of pH = 8.5–10. For the calculation of the thermodynamic constants from the titration data, we used the iterative mathematical treatment given by Albert and Serjeant.<sup>4</sup> This method takes into account overlapping ionizations and the ionic strength, which varies during the titration. The thermodynamic constants are listed in Table 1.

### Equilibrium Constant $K_T$ of the Monoprotonated Forms of 1-Methyl-*N,N*-dimethyl-*r*-1,*t*-2-cyclopro-

(4) Albert, A.; Serjeant, E. P. *The Determination of Ionization Constants*, 2nd ed.; Chapman and Hall: London, 1971.

(5) The  $pK_a$  values of 1,2-cyclobutanediamines were determined in the same way as described here for 1,2-cyclopropanediamines: Werner, M. Dissertation, University of Würzburg, 1985.

(6) Perrin, D. D. *Dissociation Constants of Organic Bases in Aqueous Solution*; Butterworths, London, 1965; and Supplement, 1972.

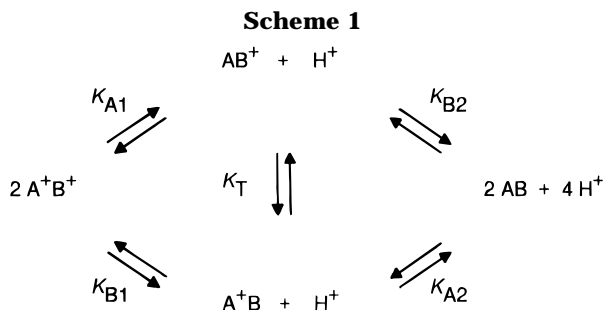
<sup>†</sup>Dedicated to Professor Lloyd M. Jackman on the occasion of his 70th birthday with great respect and affection.

<sup>®</sup> Abstract published in *Advance ACS Abstracts*, June 1, 1996.

(1) Part 5 of this series: ref 3. The results are part of the Dissertation of W. von der Saal, University of Würzburg, 1983.

(2) Present address: Boehringer Mannheim GmbH, Department of Chemistry, Sandhofer Str. 116, D-68305 Mannheim, Germany.

(3) von der Saal, W.; Quast, H. *J. Org. Chem.* **1995**, *60*, 4024.



**panediamine (*trans*-3b).** In aqueous solutions of a diamine with different protonation sites, two tautomeric monoprotinated species  $\text{A}^+\text{B}$  and  $\text{AB}^+$  exist which are connected by an equilibrium constant  $K_T$  (eq 1).<sup>7</sup> The composite, i.e. macroscopic, acidity constants  $K_1$  and  $K_2$  are related to the microscopic constants,  $K_{A1}$ ,  $K_{A2}$ ,  $K_{B1}$ , and  $K_{B2}$  by eqs 2–4<sup>7</sup> (Scheme 1).

For diamines with identical protonation sites, i.e. *cis*- and *trans*-1, *cis*-2, *trans*-4a, and *trans*-5a, the microscopic constants  $K_{A1}$  and  $K_{B1}$  are one-half of the macroscopic constant  $K_1$ , while  $K_{A2}$  and  $K_{B2}$  are twice as large as  $K_2$ . For diamines with nonequivalent amino groups, i.e. *trans*-2 and *trans*-3, it is not obvious how to partition the observed total acidities into those contributed by each of the two different ammonium groups. The four microscopic constants cannot be calculated from the macroscopic acidity data alone, because there are only three equations (eqs 2–4). For the *N,N*-dimethylcyclopropanediamine *trans*-3b, we obtained the missing information, i.e. the size of  $K_T$  (eq 1), by monitoring the change of the chemical shifts of the *N*-methyl groups in proton spectra recorded in the course of a titration.<sup>8</sup>

The *N*-methyl groups of *trans*-3b·2HBr give rise to two distinct singlets in proton spectra recorded from aqueous solutions [2.86 and 2.93 ppm ( $\text{D}_2\text{O}$ ),<sup>9</sup> 2.80 and 2.86 ppm ( $\text{H}_2\text{O}$ )]. On the basis of the ABX spectrum of the ring protons,<sup>9</sup> we assigned the *N*-methyl signals with the help of nuclear Overhauser experiments (see Experimental Section), which demonstrated that the high-field signal originates from the methylamino group at C1 of the cyclopropane ring. The chemical shifts reflect the degree of protonation of the methylamino groups and hence vary with the pH of the solution: Both decrease when KOH is added. Whereas the chemical shift of the *C*-methyl group (at C1) changes linearly and with the same slope

(7) Equations 1–4 are from ref 4.

$$K_T = [\text{A}^+\text{B}]/[\text{AB}^+] \quad (1)$$

$$K_1 = K_{A1} + K_{B1} \quad (2)$$

$$1/K_2 = 1/K_{B2} + 1/K_{A2} \quad (3)$$

$$K_1 K_2 = K_{A1} K_{B1} + K_{A2} K_{B2} \quad (4)$$

(8) Hine, J.; Via, F. A.; Jensen, J. H. *J. Org. Chem.* **1971**, *36*, 2926.

(9) von der Saal, W.; Reinhardt, R.; Seidenspinner, H.-M.; Quast, H. *Liebigs Ann. Chem.* **1994**, 569.

(10) The chemical shifts  $\Delta\delta$  are measured downfield from the signal of the free base AB:

$$\begin{aligned}
 \Delta\delta_{\text{obs}}^{\text{A}} - f_{\text{A}^+\text{B}} \Delta\delta_{\text{A}^+\text{B}}^{\text{A}} = \\
 (f_{\text{A}^+\text{B}} + f_{\text{AB}^+}) \left[ \frac{f_{\text{A}^+\text{B}}}{(f_{\text{A}^+\text{B}} + f_{\text{AB}^+})} (\Delta\delta_{\text{A}^+\text{B}}^{\text{A}} - \Delta\delta_{\text{AB}^+}^{\text{A}}) + \Delta\delta_{\text{AB}^+}^{\text{A}} \right] \quad (5)
 \end{aligned}$$

$\Delta\delta_{\text{obs}}^{\text{A}}$  denotes the observed chemical shift,  $\Delta\delta_{\text{A}^+\text{B}}^{\text{A}}$  the shift of  $\text{A}^+\text{B}^+$ ,  $\Delta\delta_{\text{AB}^+}^{\text{A}}$  the (unknown) shift of  $\text{A}^+\text{B}$ , and  $\Delta\delta_{\text{AB}^+}^{\text{A}}$  (also unknown) that of  $\text{AB}^+$ .  $f_{\text{A}^+\text{B}}$ ,  $f_{\text{A}^+\text{B}^+}$ , and  $f_{\text{AB}^+}$  denote the corresponding fractions.

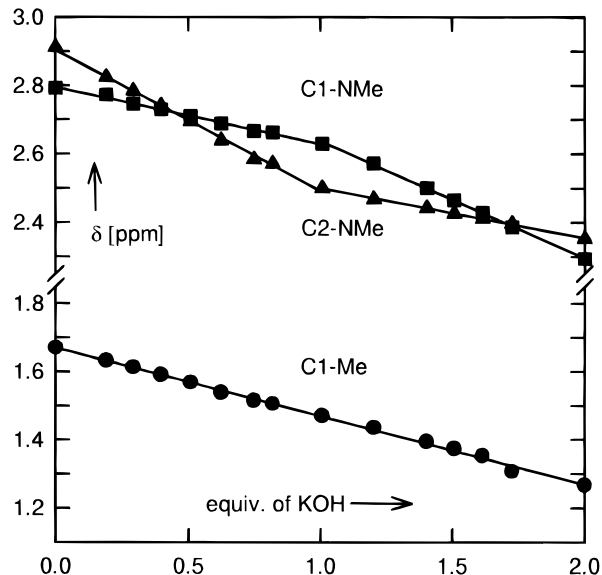


**Figure 1.** Changes of the chemical shifts (ppm) of the methyl groups at C1 (circles), at C1–N (squares), and at C2–N (triangles) in 400-MHz proton spectra of *trans*-3b·2HBr, recorded from aqueous solutions at 25 °C, upon addition of 0.1 M KOH.

over the whole range, the chemical shift of one of the *N*-methyl groups decreases faster than that of the other until exactly 1 equiv of KOH has been added. Thereafter, the chemical shifts behave inversely (Figure 1).

Obviously, the acidities of the two ammonium groups  $\text{A}^+$  and  $\text{B}^+$  are different. The methylammonium group at C1 and referred to as  $\text{A}^+$  in the following is less acidic because its chemical shift decreases more slowly on addition of KOH. For the evaluation of the tautomeric constant  $K_T$ , we considered this chemical shift first. The various forms of a diamine, differing in the degree and, in case of the monoprotinated species, the site of protonation, equilibrate rapidly. Therefore, the observed chemical shifts are the weighted averages of the chemical shifts of the equilibrating species. On this basis, Hine et al.<sup>8</sup> derived eq 5.<sup>10</sup> The sum of the fractions of the monoprotinated species, i.e.  $f_{\text{A}^+\text{B}} + f_{\text{AB}^+}$ , and the fraction of the diprotinated form ( $f_{\text{A}^+\text{B}^+}$ ) can be calculated from the macroscopic constants and the pH value.<sup>11</sup> A plot of the left side of eq 5 vs  $f_{\text{A}^+\text{B}} + f_{\text{AB}^+}$  yields a straight line through the origin with slope<sup>A</sup> (eq 6):

$$\text{slope}^{\text{A}} = \frac{f_{\text{A}^+\text{B}}}{f_{\text{A}^+\text{B}} + f_{\text{AB}^+}} (\Delta\delta_{\text{A}^+\text{B}}^{\text{A}} - \Delta\delta_{\text{AB}^+}^{\text{A}}) + \Delta\delta_{\text{AB}^+}^{\text{A}} \quad (6)$$

Second, eq 7 was derived in the same way by considering the chemical shift of the more acidic methylammonium

(11) The fractions are calculated according to the following:<sup>4</sup>

$$f_{\text{AB}} = \frac{K_1 K_2}{[\text{H}^+]^2 + K_1 [\text{H}^+] + K_1 K_2}$$

$$(f_{\text{A}^+\text{B}} + f_{\text{AB}^+}) = \frac{K_1 [\text{H}^+]}{[\text{H}^+]^2 + K_1 [\text{H}^+] + K_1 K_2}$$

$$f_{\text{A}^+\text{B}^+} = \frac{[\text{H}^+]^2}{[\text{H}^+]^2 + K_1 [\text{H}^+] + K_1 K_2}$$

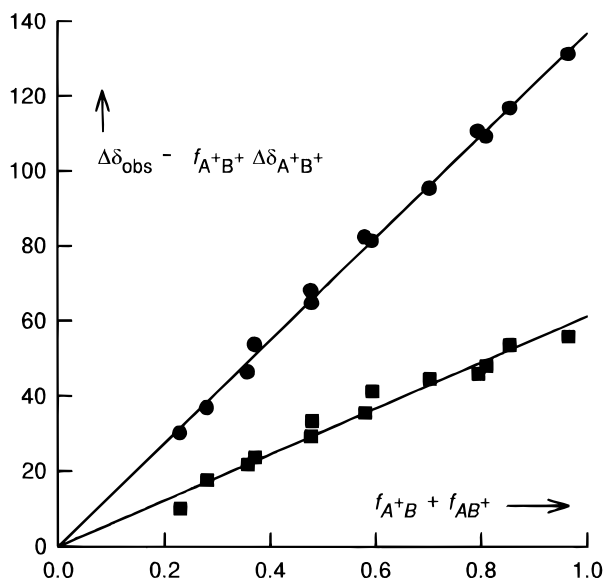


**Figure 2.**  $\Delta\delta_{obs}^A - f_{A+B}^+ \Delta\delta_{A+B}^+$  (circles) and  $\Delta\delta_{obs}^B - f_{A+B}^+ \Delta\delta_{A+B}^+$  (squares) for 1-methyl-*N,N*-dimethyl-*r*-1, *t*-2-cyclopropanediamine (*trans*-**3b**) vs the sum  $f_{A+B} + f_{AB+}$  of the fractions of the monoprotated species.

group B<sup>+</sup> at C2:

$$\text{slope}^B = \frac{f_{AB+}}{f_{A+B} + f_{AB+}} (\Delta\delta_{AB+}^B - \Delta\delta_{A+B}^B) + \Delta\delta_{A+B}^B \quad (7)$$

Plots in this manner of the experimental data yield  $\text{slope}^A = 137$  Hz and  $\text{slope}^B = 61$  Hz (Figure 2).

The tautomeric constant  $K_T$  (eq 1) is the ratio of the fractions of the monoprotated species, and hence eq 10 results.<sup>12</sup>

$$K_T = \frac{f_{A+B}}{f_{AB+}} = \frac{(\text{slope}^A - \Delta\delta_{AB+}^A)(\Delta\delta_{AB+}^B - \Delta\delta_{A+B}^B)}{(\text{slope}^B - \Delta\delta_{A+B}^B)(\Delta\delta_{A+B}^A - \Delta\delta_{AB+}^A)} \quad (10)$$

In order to be able to calculate  $K_T$  from eq 10, we needed estimates for the four unknown chemical shifts:  $\Delta\delta_{A+B}^A$ ,  $\Delta\delta_{AB+}^A$ ,  $\Delta\delta_{A+B}^B$ , and  $\Delta\delta_{AB+}^B$ .

The chemical shift of an *N*-methyl group is mainly determined by the partial charge at the nitrogen atom to which it is attached and much less by the charge of a remote ammonium group. In other words, the change in chemical shift brought about by protonation of the amino group bearing the observed methyl group ( $\Delta\delta_{A+B}^A$  or  $\Delta\delta_{AB+}^B$ ) is much larger than that caused by protonation of the remote amino group ( $\Delta\delta_{AB+}^A$  or  $\Delta\delta_{A+B}^B$ ). In order to derive a rough estimate of  $K_T$ , we neglected the effects of protonation of the remote amino groups, i.e.  $\Delta\delta_{AB+}^A = \Delta\delta_{A+B}^B = 0$ , and equated the effects of protonation of the amino groups on the chemical shift of their own methyl group, i.e.  $\Delta\delta_{A+B}^A = \Delta\delta_{AB+}^A$ . With these approximations, eq 10 yielded  $K_T$  as ratio of the slopes in Figure 2:  $K_T = 137/61 = 2.3$ .

(12) Expressions for the unknown fractions of both monoprotated forms can be derived by rewriting eqs 6 and 7:

$$f_{A+B} = \frac{(\text{slope}^A - \Delta\delta_{AB+}^A)(f_{A+B} + f_{AB+})}{(\Delta\delta_{A+B}^A - \Delta\delta_{AB+}^A)} \quad (8)$$

$$f_{AB+} = \frac{(\text{slope}^B - \Delta\delta_{A+B}^B)(f_{A+B} + f_{AB+})}{(\Delta\delta_{AB+}^B - \Delta\delta_{A+B}^B)} \quad (9)$$

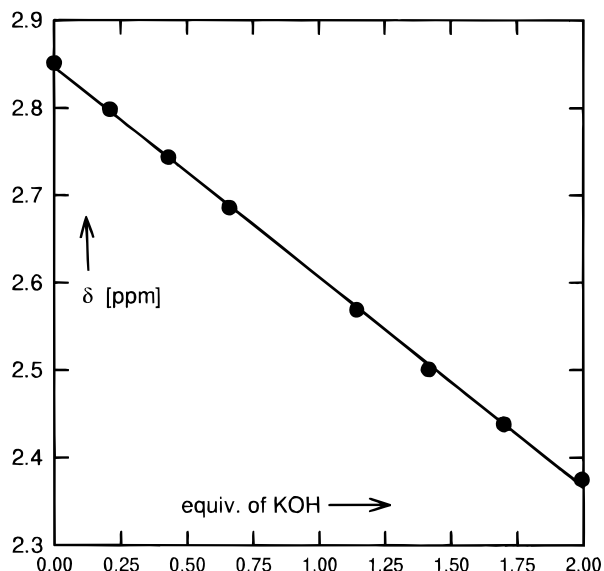


**Figure 3.** Chemical shifts (ppm) of the *N*-methyl groups in the proton spectra recorded from aqueous solutions of *trans*-*N,N*-dimethylcyclopropanediammonium dibromide (*trans*-**1b**·2HBr) at 25 °C after addition of 0.1 M KOH.

In order to obtain a more realistic value for  $K_T$ , we derived the effect of remote protonation from a model compound. Hine et al.<sup>8</sup> reported that, in a 60-MHz proton spectrum, the methoxy signal of 2-methoxyethanamine shifts by 2 Hz upon protonation of the amino group. We employed this value (13 Hz at 400 MHz) as an estimate for the effect of protonation of the remote amino group, because the observed protons are separated by five bonds from the protonation site in both, 2-methoxyethanamine and *trans*-**3b**. In addition, we assumed the protonation shifts brought about by the remote amino groups to be the same for A and B:

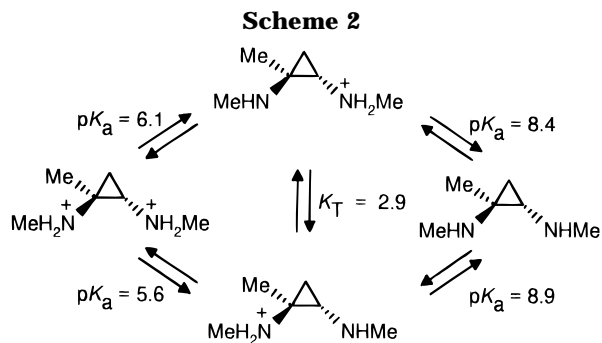
$$\Delta\delta_{AB+}^A = \Delta\delta_{A+B}^B = 13 \text{ Hz} \quad (11)$$

Second, we considered that, most probably,  $\Delta\delta_{A+B}^A$  is different from  $\Delta\delta_{AB+}^B$ . To account for this difference, we assumed that the shift resulting from protonation of the observed methylamino group is the same whether (right sides of eq 12 and 13) or not (left sides of eq 12 and 13) the remote amino group is already protonated:

$$\Delta\delta_{A+B}^A = \Delta\delta_{A+B+}^A - \Delta\delta_{AB+}^A \quad (12)$$

$$\Delta\delta_{AB+}^B = \Delta\delta_{A+B+}^B - \Delta\delta_{A+B}^B \quad (13)$$

The validity of this approximation may be questioned. One may speculate, for instance, that on protonation of an amino group the cyclopropane ring may undergo structural changes that influence the chemical shift of the *N*-methyl groups. Protonation of the observed amino group will thus give rise to different effects if the remote amino group is protonated or not. We addressed this question with the help of the symmetrical cyclopropanediammonium dibromide *trans*-**1b**·2HBr as a model. A plot of the chemical shift of the *N*-methyl groups vs the amount of added KOH yielded a straight line (Figure 3). This proved that the assumptions made in eqs 12 and 13 are valid. Otherwise one would observe a point of inflection in the line of Figure 3 after the addition of 1 equiv of KOH.



Using the experimental values for  $\Delta\delta_{A+B^+}^A$  (199 Hz) and  $\Delta\delta_{A+B^+}^B$  (223 Hz) and the estimated value for  $\Delta\delta_{AB^+}^A$  (13 Hz), we calculated  $K_T = 2.9$  (eq 14<sup>13</sup>). If the effect of protonation of the remote amino group was neglected, i.e.  $\Delta\delta_{AB^+}^A$ , then  $K_T = 2.5$ .

With the knowledge of the tautomeric constant  $K_T$ , a detailed picture of the equilibria can be derived including the calculation of the microscopic acidity constants (Scheme 2).

**Kinetic Measurements of the Conversion of *trans*-3a·2HBr in Aqueous Buffer Solutions.** The conversion of *trans*-3a·2HBr into **8** in various buffer solutions at 35 °C was monitored by proton spectroscopy with the help of the signals of the methyl groups. The results are listed in Table 2.

The reaction started after an initiation period, which lasted approximately 1 h at pH = 5.8 and 25 °C,<sup>3</sup> but only a few minutes at pH = 8 and 35 °C. Once a small amount of **8** had arisen, the rate increased considerably. These observations were indicative of a mechanism involving a slow, "spontaneous" conversion of *trans*-3a into **8** with a rate constant  $k_1$  followed by a rapid autocatalytic conversion into **8** with a rate constant  $k_2$ .<sup>15</sup> This kinetic scheme yielded eq 15 and its integrated form, eq 16, where  $[AB_t]$  denotes the total amount of the cyclopropanediamine present, i.e. the free base  $[AB]$ , the monoprotonated forms  $[A^+B]$  and  $[AB^+]$ , and the cyclopropanediammonium ion  $[A^+B^+]$ , and  $[C]$  the concentration of **8** which is the catalyst.

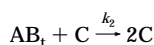
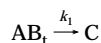
If the catalyst is absent at the onset ( $[C]_0 = 0$ ), eq 16 is reduced to eq 17. A nonlinear fit<sup>14</sup> of the data in Figure

(13) The combination of eqs 10–13 yields eq 14:

$$K_T = \frac{(\text{slope}^A - \Delta\delta_{AB^+}^A)(\Delta\delta_{A+B^+}^B - 2\Delta\delta_{AB^+}^A)}{(\text{slope}^B - \Delta\delta_{AB^+}^B)(\Delta\delta_{A+B^+}^A - 2\Delta\delta_{AB^+}^B)} \quad (14)$$

(14) The program used was SigmaPlot from Jandel Scientific, D-40699 Erkrath, Germany.

(15) Moore, J. W.; Pearson, R. G. *Kinetics and Mechanism*, J. Wiley and Sons: New York, 1981; p 26. The kinetic scheme and the equations are as follows:



$$\frac{-d[AB_t]}{dt} = k_1[AB_t] + k_2[AB_t][C] \quad (15)$$

$$[AB_t]_t = \frac{[AB_t]_0\{k_1 + k_2([AB_t]_0 + [C]_0)\}}{k_2[AB_t]_0 + (k_1 + k_2[C]_0)e^{\{k_1 + k_2([AB_t]_0 + [C]_0)\}t}} \quad (16)$$

$$[AB_t]_t = \frac{[AB_t]_0(k_1 + k_2[AB_t]_0)}{k_2[AB_t]_0 + k_1e^{\{k_1 + k_2[AB_t]_0\}t}} \quad (17)$$

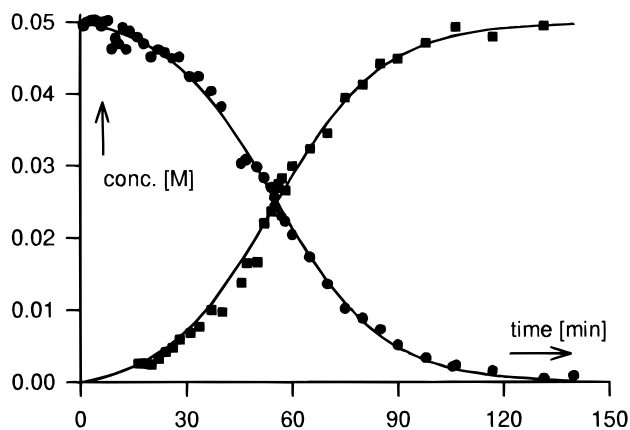


**Figure 4.** Conversion of 1-methyl-*r*-1,*t*-2-cyclopropanediammonium dibromide (*trans*-3a·2HBr, circles, 0.05 M solution in 0.5 M phosphate buffer of pH = 7.4 at 35 °C, run 8) into 4-aminobutan-2-one (**8**, squares). The curves were drawn by a nonlinear fit<sup>14</sup> of the data to eq 17.

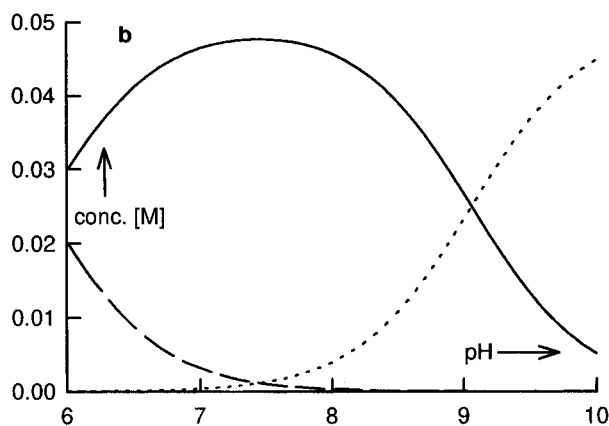
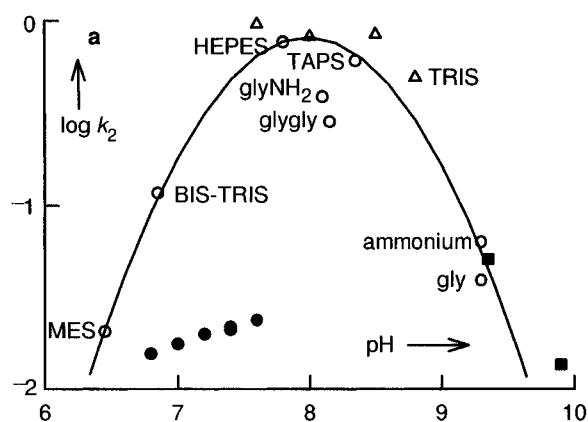


**Figure 5.** (a) Variation of the second-order ("autocatalytic") rate constant  $k_2$  with the pH value in various buffer solutions: open symbols, amine buffers; filled circle, phosphate buffers; filled square, borate buffers. The second-order regression curve, calculated from the data of the amine buffers, is shown. The data of runs 2, 19, 21, and 23 in Table 2 have been omitted. (b) Variation of the composition of a 0.05 M solution of 1-methyl-*r*-1,*t*-2-cyclopropanediammonium dibromide (*trans*-3a·2HBr) between pH = 6 and 10: dashed line, concentration of the dication *trans*-3a·2H<sup>+</sup>; solid line, sum of the concentrations of the two monoprotonated forms ( $[A^+B] + [AB^+]$ ); dotted line, free base *trans*-3a.<sup>17</sup>

4 (run 8) to eq 17 yielded the rate constants  $k_1 = (3.1 \pm 0.2) \times 10^{-5} \text{ s}^{-1}$  and  $k_2 = (2.09 \pm 0.06) \times 10^{-2} \text{ L mol}^{-1} \text{ s}^{-1}$ .<sup>16</sup>

**Table 2. Experimental Conditions and Kinetic Results of the Conversion of 1-Methyl-*r*-1,*t*-2-cyclopropanediammonium Dibromide (*trans*-**3a**·2HBr, 0.05 M, 35 °C) into 4-Aminobutan-2-one (**8**) in Aqueous Buffer Solutions<sup>a</sup>**

run	buffer <sup>b</sup>	[HB] <sup>c</sup>	[B <sup>-</sup> ] <sup>d</sup>	[KCl] <sup>e</sup>	pH	<i>f</i>	<i>g</i>	<i>h</i>	10 <sup>5</sup> <i>k</i> <sub>1</sub> (s <sup>-1</sup> )	10 <sup>2</sup> <i>k</i> <sub>2</sub> (L mol <sup>-1</sup> s <sup>-1</sup> )
1	MES	0.20	0.30	1.20	6.4–6.5	2	B	35	7.8 ± 0.7	2.0 ± 0.1
2	MES	0.40	0.60	0.90	6.4–6.5	1	B	30	11.8 ± 1.2	3.0 ± 0.2
3	BIS-TRIS	0.20	0.30	1.20	6.8–6.9	0.5	B	11	48 ± 6	11.7 ± 1.0
4	phosphate	0.15	0.35	0.30	6.8	3	A	50	1.17 ± 0.03	1.55 ± 0.01
5	phosphate	0.10	0.40	0.20	7.0	3	A	50	1.23 ± 0.06	1.76 ± 0.03
6	phosphate	0.075	0.425	0.15	7.2	2	A	60	1.48 ± 0.04	1.99 ± 0.02
7	phosphate	0.05	0.45	0.10	7.4	2	A	60	1.29 ± 0.05	2.16 ± 0.02
8	phosphate	0.05	0.45	0.10	7.4	2	B	50	3.1 ± 0.2	2.09 ± 0.06
9	phosphate	0.025	0.475	0.05	7.6	2	A	50	4.2 ± 0.2	2.38 ± 0.04
10	TRIS	0.40	0.10	0.70	7.5–7.8	0.1	C	10	2.3 ± 0.7	96 ± 4
11	HEPES	0.20	0.30	1.20	7.8	0.1	C	10	5.7 ± 1.1	76 ± 3
12	TRIS	0.30	0.20	0.90	7.9–8.1	0.1	C	10	5.7 ± 0.3	82 ± 7
13	glyNH <sub>2</sub>	0.20	0.30	1.00	8.1–8.2	0.1	C	10	6.1 ± 1.6	39 ± 3
14	glygly	0.20	0.30	1.20	8.1–8.2	0.1	C	10	14 ± 2	28.4 ± 1.4
15	TAPS	0.20	0.30	1.20	8.3–8.4	0.1	C	10	3.1 ± 0.7	60 ± 2
16	TRIS	0.15	0.35	1.20	8.4–8.6	0.1	C	10	1.3 ± 0.2	84 ± 2
17	TRIS	0.10	0.40	1.30	8.7–8.9	0.1	C	10	4.0 ± 0.5	49.4 ± 1.0
18	gly	0.17	0.33	1.17	9.2–9.4	1	A	10	7 ± 4	3.9 ± 1.1
19	gly	0.17	0.33	1.17	9.2–9.4	1	B	30	7.4 ± 0.5	4.2 ± 0.2
20	NH <sub>4</sub> Cl	0.025	0.475	0.75	9.2–9.4	1	A	30	7.1 ± 1.0	6 ± 3
21	boric acid	0.25	0.25	1.25	9.0–9.5	1	B	20	2.8 ± 0.5	5.9 ± 0.3
22	boric acid	0.20	0.30	1.20	9.2–9.5	1	A	30	7.4 ± 0.7	5.1 ± 0.2
23	boric acid	0.20	0.30	1.20	9.2–9.5	1	B	30	13.6 ± 1.6	4.0 ± 0.4
24	boric acid	0.10	0.40	1.10	9.8–10	2	B	50	3.5 ± 0.1	1.36 ± 0.03

<sup>a</sup> The rate constants *k*<sub>1</sub> and *k*<sub>2</sub> (± asymptotic standard errors) were obtained by nonlinear fits<sup>14</sup> of the data to eq 16.<sup>15</sup> <sup>b</sup> Concentration 0.5 M, ionic strength 1.5, abbreviations see Experimental Section. <sup>c</sup> Concentration of the acidic component of the buffer solution [M]. <sup>d</sup> Concentration of the basic component of the buffer solution. <sup>e</sup> Concentration of KCl added for the adjustment of the ionic strength. <sup>f</sup> Duration of the experiment (h). <sup>g</sup> Method for determination of the concentrations; A, sum of *trans*-**3a** and **8** = 100%; B, comparison of the signal heights of *trans*-**3a** and standard (sodium (trimethylsilyl)propanesulfonate); C, comparison of the signal heights of *trans*-**3a** with the height of the same signal during the initial 2 min. <sup>h</sup> Number of data used in the calculation.

**Catalysis by Buffers.** The rate constants *k*<sub>2</sub> depended on both pH and nature of the buffer. They reached a maximum around pH 8 (Figure 5a). Amine buffers were more effective than phosphate buffers. This is quite evident when the value of *k*<sub>2</sub> obtained from a phosphate buffer at pH = 6.8 is compared with that from a BIS-TRIS buffer of the same pH (runs 3 and 4 in Table 2). The acceleration of the autocatalytic step by amine buffers is even more clearly demonstrated by a comparison of the results obtained from a phosphate buffer and a TRIS buffer of pH 7.6 (runs 9 and 10 in Table 2). In a solution of the latter, the conversion was complete within 10 min, whereas several hours were required in a solution of the former. The rate constants *k*<sub>2</sub> also depended on the concentration of the buffer. A 2-fold increase to a concentration of 1 M accelerated the reaction considerably (runs 1 and 2 in Table 2). These observations indicate that the buffer (one or both components) participates in the rate-determining step of the catalytic cycle. The buffers act as general acid/base catalysts but not as nucleophilic catalysts. This is inferred from the observation that tertiary amine buffers (HEPES, run 11

in Table 2) gave rise to very similar rates as primary amine buffers (TRIS, run 10).

In the experiments performed in phosphate buffer solutions (runs 4–9 in Table 2), the rate constant *k*<sub>2</sub> increases with increasing pH (6.8 → 7.6). Within this pH range, the concentrations of both dication *trans*-**3a**·2H<sup>+</sup> and free base *trans*-**3a** are low. The main species present are the two monocations *trans*-**3a**·H<sup>+</sup>, i.e. A<sup>+</sup>B and AB<sup>+</sup>.<sup>17</sup> Furthermore, the concentration of these monocations is nearly constant in this pH range (Figure 5b). The related *N,N'*-dimethyl monocations *trans*-**3b**·H<sup>+</sup> have a tautomeric constant *K*<sub>T</sub> of 2.9. We expect a similar behavior for *trans*-**3a**·H<sup>+</sup> and hence that the concentration of A<sup>+</sup>B is always larger than that of AB<sup>+</sup>.

The species involved in the rate-determining step cannot be a combination of A<sup>+</sup>B<sup>+</sup> and the general acid H<sub>2</sub>PO<sub>4</sub><sup>-</sup>,<sup>18</sup> because this is not compatible with the maximum of the rate constant near pH = 8. The same is true for a combination of the monocations and H<sub>2</sub>PO<sub>4</sub><sup>-</sup>, because the concentration of the monocations remains constant between pH = 6.8 and 7.6, and the concentration of H<sub>2</sub>PO<sub>4</sub><sup>-</sup> declines, whereas *k*<sub>2</sub> increases. A combination of H<sub>2</sub>PO<sub>4</sub><sup>-</sup> and the free base AB was found to be consistent with the experimental results. The product of the second-order rate constant *k*<sub>2</sub> and the total concentration of *trans*-**3a** can be replaced by the product of a new, third-order rate constant *k*<sub>3</sub>, and the concentrations of the general acid H<sub>2</sub>PO<sub>4</sub><sup>-</sup> and the free base AB (eq 18). Division of eq 18 by [AB]<sub>t</sub> affords an expression

(16) It may be assumed that the "spontaneous" ring opening does not take place at all (*k*<sub>1</sub> = 0), but that a small amount of catalyst C is present at the onset ([C]<sub>0</sub> > 0). Thus, eq 16 collapses to

$$[\text{AB}]_t = \frac{[\text{AB}]_0(k_2[\text{C}]_0 + k_2[\text{AB}]_0)}{k_2[\text{AB}]_0 + k_2[\text{C}]_0 e^{(k_2[\text{C}]_0 + k_2[\text{AB}]_0)t}}$$

which is identical with eq 17 if *k*<sub>1</sub> in eq 17 is replaced by *k*<sub>2</sub>[C]<sub>0</sub>. Consequently, a nonlinear fit of the data of Figure 4 to this equation gives the same value for *k*<sub>2</sub> as before and an estimate for [C]<sub>0</sub> = 0.0014 ± 0.0006 M. Because the experimental design would not have allowed detection of a catalyst at such a low concentration, we cannot rule out that some **8** or another ketone may have been present already at the beginning. Two recrystallizations of *trans*-**3a**·2HBr from methanol did not affect the initiation phase, however. Therefore, eq 17 seems to describe properly the conversion vs time curve, and we report in Table 2 rate constants *k*<sub>1</sub> but not hypothetical initial concentrations of a catalyst.

(17) The composition of the solutions at pH 6–10 (Figure 5b) was calculated from the ionization constants *K*<sub>1</sub> and *K*<sub>2</sub> in the eq of footnote 11.

(18) The concentrations of the general acid H<sub>2</sub>PO<sub>4</sub><sup>-</sup> and the general base HPO<sub>4</sub><sup>2-</sup> were slightly different from those used for the preparation of the buffer solutions, because addition of *trans*-**3a**·2HBr gave rise to an increase of the pH value by 0.2–0.4. Therefore, we measured the pH values and used the concentrations given for the measured pH values by Green: Green, A. A. *J. Am. Chem. Soc.* **1933**, *55*, 2331.

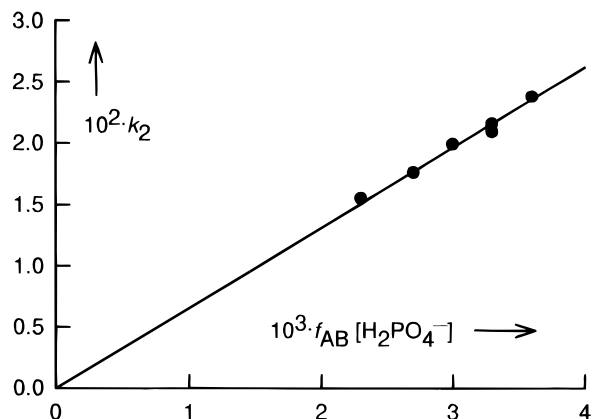


**Figure 6.** Variation of the rate constant  $k_2$  with the product of the concentration of the general acid  $\text{H}_2\text{PO}_4^-$  and the fraction  $f_{\text{AB}}$  of the free base *trans*-**3a**.

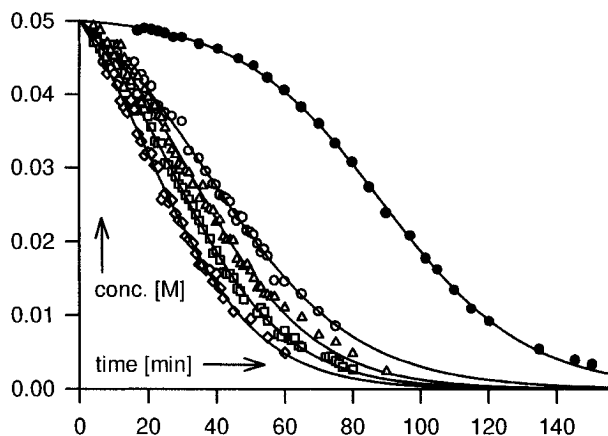


**Figure 7.** Concentration vs time curves for reactions of *trans*-**3a**·2HBr (0.05 M solutions in 0.5 M phosphate buffer of pH = 6.8 at 35 °C) in the absence (filled circles) and in the presence of acetone (open symbols; circles, 2 mM acetone; triangles, 3 mM; squares, 4 mM; diamonds, 5 mM).

for a straight line through the origin with a slope  $k_3$  (eq 19).

$$k_2[\text{AB}]_t = k_3[\text{H}_2\text{PO}_4^-][\text{AB}] \quad (18)$$

$$k_2 = k_3[\text{H}_2\text{PO}_4^-]f_{\text{AB}} \quad (19)$$

A plot of experimentally determined rate constants  $k_2$  vs the product of the concentration of the general acid  $\text{H}_2\text{PO}_4^-$  and the fraction of the free base ( $f_{\text{AB}}$ ) does indeed yield a straight line through the origin (Figure 6) with a slope  $k_3 = 6.5 \text{ L}^2 \text{ mol}^{-2} \text{ s}^{-1}$ .

**Catalysis by Acetone and Butanone.** We have shown previously that the addition of minute amounts of a solution, in which *trans*-**3a**·2HBr had completely decomposed to afford **8**, to a freshly prepared solution of *trans*-**3a**·2HBr enhances the reaction rate dramatically<sup>3</sup> (Scheme 3). The addition of ammonium chloride has no effect. Even the use of ammonium chloride as component of a buffer (run 20 in Table 2) does not yield a rate constant which differs significantly from those obtained with glycine (run 19) or borate (run 21) buffers. Therefore, we assumed that the carbonyl moiety of **8** but not its amino group participates in the rate-determining step. Other ketones should hence behave similarly. Acetone (Figure 7) and butanone (Figure 8) do indeed cause a concentration-dependent increase of the rates. Therefore,

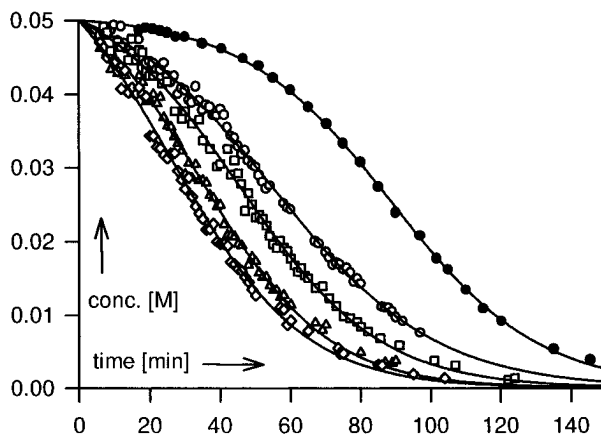
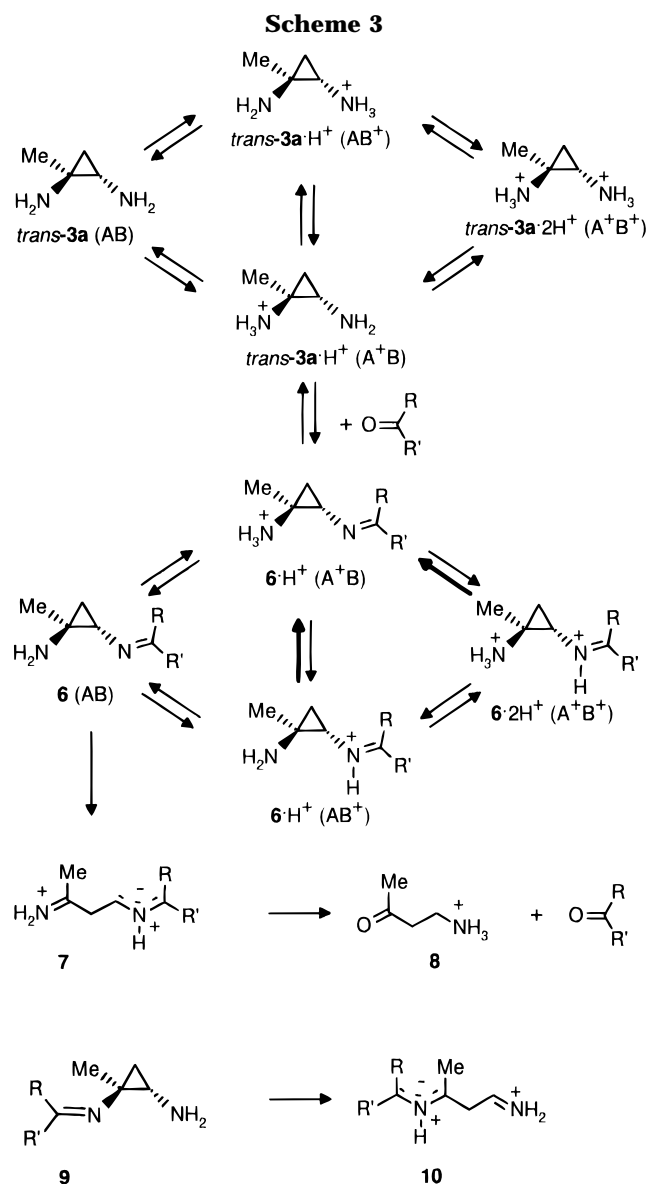


**Figure 8.** Concentration vs time curves for reactions of *trans*-**3a**·2HBr (0.05 M solutions in 0.5 M phosphate buffer of pH = 6.8 at 35 °C) in the absence (filled circles) and in the presence of butanone (open symbols; circles, 2 mM butanone; triangles, 3 mM; squares, 5 mM; diamonds, 8 mM).



the previous kinetic scheme was extended to include the reaction with ketones (eq 20).<sup>19</sup>

We defined a combined rate constant  $k_4$  (eq 21) which depends on the chosen, constant ketone concentration.

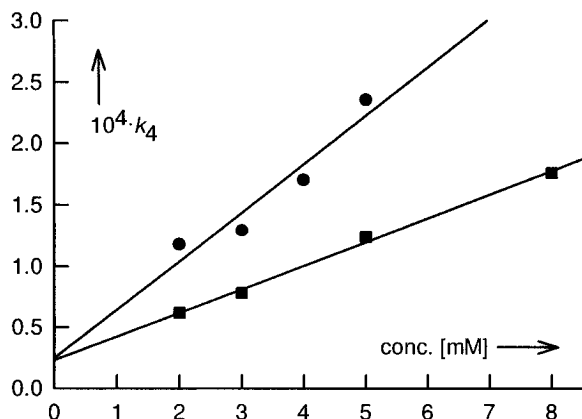


**Figure 9.** Dependence of the rate constant  $k_4$  on the concentration of acetone (circles) and butanone (squares) according to eq 21.

**Table 3.** Rate Constants  $k_1$  and  $k_2$  ( $\pm$  Asymptotic Standard Error) Obtained by Nonlinear Fits of the Data of Figures 7 and 8 to the Integrated Form of Eq 22

ketone (mol L <sup>-1</sup> )	acetone		butanone			
	run	$10^4 k_4$ (s <sup>-1</sup> )	$10^2 k_2$ (L mol <sup>-1</sup> s <sup>-1</sup> )	run	$10^4 k_4$ (s <sup>-1</sup> )	$10^2 k_2$ (L mol <sup>-1</sup> s <sup>-1</sup> )
0.002	25	1.18 $\pm$ 0.06	1.31 $\pm$ 0.06	29	0.62 $\pm$ 0.02	1.31 $\pm$ 0.03
0.003	26	1.29 $\pm$ 0.04	1.62 $\pm$ 0.05	30	0.78 $\pm$ 0.03	1.51 $\pm$ 0.05
0.004	27	1.70 $\pm$ 0.04	1.64 $\pm$ 0.04			
0.005	28	2.36 $\pm$ 0.08	1.61 $\pm$ 0.08	31	1.24 $\pm$ 0.05	1.58 $\pm$ 0.06
0.008				32	1.76 $\pm$ 0.07	1.44 $\pm$ 0.07

Subsequently, we converted eq 20 into a rate equation (eq 22) which is identical with eq 15. Thus, the integrated form of eq 15, i.e. eq 16, could be employed, and it yielded the rate constants  $k_1$  and  $k_2$  listed in Table 3.

$$k_4 = k_1 + k_{\text{ketone}}[\text{ketone}] \quad (21)$$

$$\frac{-d[\text{AB}_t]}{dt} = k_1[\text{AB}_t] + k_2[\text{AB}_t][\text{C}] \quad (22)$$

The rate constant  $k_2$  remains essentially unchanged, while  $k_4$  increases with increasing concentrations of the ketones as expected. According to eq 21, plots of  $k_4$  vs the ketone concentration afford straight lines with a common intercept, which equals  $k_1$ , and with slopes corresponding to  $k_{\text{ketone}}$  (Figure 9). The slope  $k_{\text{ketone}}$  is  $4.0 \times 10^{-2}$  L mol<sup>-1</sup> s<sup>-1</sup> for acetone and  $1.9 \times 10^{-2}$  L mol<sup>-1</sup> s<sup>-1</sup> for butanone. The intercept is  $2.4 \times 10^{-5}$ , a value which is virtually identical with  $k_1$  obtained in the uncatalyzed reactions. The observation that  $k_{\text{ketone}}$  of acetone is twice as large as  $k_2$ , the rate constant in the absence of acetone, shows that acetone catalyzes more efficiently than **8**. Butanone is approximately as effective as **8**.

## Discussion

The relative configuration of the vicinal ammonium groups at the cyclopropane ring strongly affects the  $pK_a$  values. *cis*-1,2-Cyclopropanediammonium ions are distinctly more acidic than the *trans* isomers ( $\Delta pK_{a1} = pK_{a1}(\text{trans}) - pK_{a1}(\text{cis}) = 1.6$  to 1.7). The (more flexible) 1,2-cyclobutanediammonium ions ( $\Delta pK_{a1} = 1.3$ )<sup>5</sup> and 1,2-cyclohexanediammonium ions ( $\Delta pK_{a1} = 0.3$ )<sup>6</sup> show the same behavior but to a lesser extent. This difference between the diastereomers can be traced back to the proximity of the positive charges in the *cis* diammonium ions. The monoprotonated form of a *cis*-1,2-cyclopro-

panediamine may be stabilized by an intramolecular hydrogen bond, which results in a decrease of  $pK_{a1}$  and an increase of  $pK_{a2}$  as observed. *N*-Methyl groups reduce  $pK_{a1}$  further by 0.6 for *cis* isomers and 0.2 to 0.3 for *trans* isomers. This contrasts to the methyl group effect in the case of the 1,2-ethanediammonium ion whose  $pK_{a1}$  is increased by *N*-methyl groups by 0.6.<sup>6</sup> *N*-Methyl groups affect  $pK_{a2}$  much less and in a way which does not offer an obvious consistent pattern.

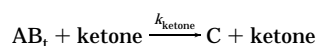
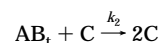
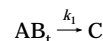
The effect of a methyl group at C1 is revealed by a comparison of the microscopic constants of *trans*-**1b**·2HBr (5.95, 8.43) with those of *trans*-**3b**·2HBr (Scheme 2). The methyl group decreases the acidity of the geminal and increases that of the vicinal ammonium group.

**Mechanism of the Autocatalytic and the Ketone-Catalyzed Ring Opening.** The nucleophilic reactivity of amines toward carbonyl compounds parallels the basicity of the amines.<sup>20</sup> The free base *trans*-**3a** is hence the most reactive species. The amino groups of both monocations are less basic by 2–3 orders of magnitude. Their reactivities are expected to be 50–100 times smaller<sup>20</sup> but their concentrations are 10–100 times larger than that of the free base (Figure 5b). Therefore, *trans*-**3a** and its monocations *trans*-**3a**·H<sup>+</sup> may react with similar rates to afford imines. Due to the small equilibrium constants for the formation of imines in aqueous solution,<sup>21</sup> direct observation of **6** and **9** by NMR spectroscopy was impossible. Similar systems of acid/base equilibria as for *trans*-**3a** exist for the imines **6** and **9**. Again, the monoprotonated forms predominate but their tautomeric equilibria are shifted far to the ammonium ions because iminium ions are more acidic by 3 orders of magnitude than the corresponding ammonium ions.<sup>22</sup> For the same reason, the dications are almost totally absent and the proportions of the free bases are larger.

Most probably, it is the free base **6**, which is attacked by the general acid with concomitant ring opening to form the azomethine ylide **7** in the rate-limiting step. The azomethine ylide **7** is hydrolyzed to furnish the amino ketone **8**. As shown by the almost quantitative yield of **8** (95–98%), the analogous ring cleavage of the isomeric imine **9**, whose product **10** would be hydrolyzed to afford aldehydes does not play a significant role. Only very small amounts of aldehydes are actually formed in a minor side reaction. These eventually yield the pyrroles which are detected by the Ehrlich test.<sup>3</sup>

If ring opening of **6** is the *slow* step, then **6** would have to be formed from *trans*-**3a** and a ketone in a *fast* equilibrium whose constant is smaller for an encumbered

(19) The kinetic scheme is



and eq 20 is

$$\frac{-d[\text{AB}_t]}{dt} = k_1[\text{AB}_t] + k_2[\text{AB}_t][\text{C}] + k_{\text{ketone}}[\text{AB}_t][\text{ketone}]$$

(20) Hine, *J. Acc. Chem. Res.* **1978**, *11*, 1.

(21) The equilibrium constant for the imine formation from methanamine and acetone in water is 11.5 at 25 °C: Williams, A.; Bender, M. L. *J. Am. Chem. Soc.* **1966**, *88*, 2508. On the basis of this constant, the concentration of the imines would reach a maximum of 0.13 mM, when the reaction had proceeded halfway.

(22) Jencks, W. P. *Acc. Chem. Res.* **1976**, *9*, 425.

ketone and hence also the rate of the reaction that is catalyzed by this ketone. This is indeed borne out by the experiments.

The kinetic measurements do not unequivocally prove, of course, that the rate-determining step is truly the general acid-catalyzed ring opening of **6**. (1) The reaction of a general base with one or both monocations **6**(A<sup>+</sup>B) and **6**(AB<sup>+</sup>) cannot be distinguished on the basis of kinetics from the reaction of a general acid with the free base **6** advocated above.<sup>23</sup> (2) In the reaction of a weakly basic amine with a ketone, the dehydration of the intermediate adduct is catalyzed by acids and may be rate-limiting.<sup>24</sup> In this case, the rate law for the *ketone-catalyzed* reaction would be eq 23.<sup>25</sup> One would expect encumbered ketones to react more slowly, as is indeed observed. Therefore, we cannot exclude that formation of the imine **6** is rate-limiting.

### Concluding Remarks

The p*K*<sub>a</sub> values of the 1,2-cyclopropanediammonium dibromides **1–5** and the equilibrium constant of the two monocations of *trans*-**3b** help to interpret reactions in aqueous solution.<sup>3</sup> Furthermore, the data may serve to improve computational methods for the prediction of p*K*<sub>a</sub> values of small diamines. Such methods have recently regained much interest in chemistry and biology.<sup>26</sup> Up to now, the mathematical models had to include assumptions about the principal conformations, because p*K*<sub>a</sub> values of only flexible molecules were available.<sup>27</sup>

The conversion of *trans*-**3a**·2HBr into **8** in aqueous buffer solutions of pH 6.5–10 is an autocatalytic process. In addition, it is catalyzed by acetone or butanone and is subject to general acid/base catalysis, particularly by amine buffers. The reactive species is an imine **6**, which opens the ring to an intermediate **7** possessing both an azomethine ylide<sup>28</sup> and an imine moiety.

The proposed mechanism may also operate in the decomposition of other 1,2-cyclopropanediamines which commences in aqueous phosphate buffers only after a similar initiation period. Their products are too unstable to be observed, however. Aldehydes do not catalyze the conversion of *trans*-**3a** into **8** but do furnish pyrroles. Probably, this reaction also involves azomethine ylides of type **7** which, instead of being hydrolyzed, close a five-membered ring. This formation of pyrroles from 1,2-cyclopropanediamines will be dealt with in a forthcoming paper.

(23) Lowry, T. H.; Richardson, K. S. *Mechanisms and Theory in Organic Chemistry*, 2nd ed.; Harper and Row: New York 1981, p 608. The combination of the acidity constants of the monocations *trans*-**3a**·H<sup>+</sup> and H<sub>2</sub>PO<sub>4</sub><sup>-</sup> with eq 18 results in a rate equation for the reaction of the general base HPO<sub>4</sub><sup>2-</sup> with the monocations *trans*-**3a**·H<sup>+</sup>.

(24) Jencks, W. P. *Catalysis in Chemistry and Enzymology*; McGraw-Hill: New York, 1969; p 490.

(25)

$$-\frac{d[AB_1]}{dt} = k_{\text{imine}}[AB_1][HB][\text{ketone}] \quad (23)$$

(26) For a review, see: Honig, B.; Nicholls, A. *Science* **1995**, *268*, 1144.

(27) Potter, M. J.; Gilson, M. K.; McCammon, J. A. *J. Am. Chem. Soc.* **1994**, *116*, 10298.

(28) Reviews on azomethine ylides: Tsuge, O.; Kanemasa, S. *Adv. Heterocycl. Chem.* **1989**, *45*, 231. Claus, P. K. In *Houben-Weyl, Methoden der Organischen Chemie*, 4th ed.; Klamann, D., Hagemann, H., Eds.; Thieme: Stuttgart, 1990; Vol. E14b, Part 1, p 74. Vedejs, E. In *Advances in Cycloaddition*; Curran, D. P., Ed.; Jai Press: Greenwich, CT, 1988; Vol. 1, Kanemasa, S.; Tsuge, O. In *Advances in Cycloaddition*; Curran, D. P., Ed.; Jai Press: Greenwich, CT, 1993; Vol. 3. For more recent work, see for example: Ardill, H.; Grigg, R.; Malone, J. F.; Sridharan, V.; Thomas, W. A. *Tetrahedron* **1994**, *50*, 5067 and references cited therein.

### Experimental Section

**<sup>1</sup>H NMR Spectra.** Spectrometers used were WM 400 of Bruker and EM 390 of Varian. Sodium 3-(trimethylsilyl)propanesulfonate was used as internal standard because its shift does not change with the pH value of the solution.<sup>29</sup>

**Materials.** The 1,2-cyclopropanediammonium dibromides were recrystallized from methanol/water (95:5) and dried in vacuo over P<sub>2</sub>O<sub>5</sub> for 1 d. The water employed in the experiments was distilled twice in an all-quartz apparatus and heated to 100 °C under N<sub>2</sub> for 5 min prior to use. N<sub>2</sub> used as inert gas was bubbled through concentrated aqueous KOH and subsequently through water. Standard buffer solutions were purchased from Riedel-de Haën, 0.100 M KOH from Merck. Buffers were purchased from Sigma: 2-(morpholin-4-yl)ethanesulfonic acid (MES), 2-[N,N-bis(2-hydroxyethyl)amino]-2-(hydroxymethyl)propane-1,3-diol (BIS-TRIS), 2-amino-2-(hydroxymethyl)propane-1,3-diol (TRIS), 2-[4-(2-hydroxyethyl)-piperazin-1-yl]ethanesulfonic acid (HEPES), 3-[2-hydroxy-1,2-bis(hydroxymethyl)ethylamino]propane-1-sulfonic acid (TAPS), glycine (gly), glycylglycine (glygly), and glycylamide hydrochloride (glyNH<sub>2</sub>).

Solutions (0.5 M) of MES, HEPES, TAPS, glycine, glycylamide hydrochloride, glycylglycine, NH<sub>4</sub>Cl, and boric acid were prepared by dissolving the acidic forms and KCl in water and addition of the appropriate amounts of 1 M NaOH and water. Solutions of TRIS and BIS-TRIS buffers (0.5 M) were prepared from the basic forms, KCl, and 1 M HCl. Phosphate buffer (0.5 M) was prepared from KH<sub>2</sub>PO<sub>4</sub>, Na<sub>2</sub>HPO<sub>4</sub>, and KCl (Table 2).

**pH Values** were measured with a glass electrode EM 125 containing an Ag/AgCl/KCl (3M) standard electrode and a digital pH meter, both of Deutsche Metrohm GmbH, D-70794 Filderstadt, Germany. Prior to each measurement in the range of pH 3–7, the electrode was calibrated at 25 °C with a phosphate (pH = 6.865) and a potassium phthalate buffer (pH = 4.008). For the range between pH 7 and 10 the phosphate buffer (pH = 6.865) and a sodium tetraborate buffer (pH = 9.180) were employed.

**Determination of p*K*<sub>a</sub> Values.** Glass electrode, standard buffer solutions, and the apparatus containing 50.0 mL water were kept for 5 h at 25.0 ± 0.1 °C. The apparatus consisted of a 100-mL three-necked flask, magnetic stirrer, the glass electrode, and a calibrated 5-mL glass buret connected to a stainless steel syringe, and the whole was flushed with N<sub>2</sub> for 0.5 h. A positive pressure of N<sub>2</sub> was maintained throughout. The buret was filled with 0.100 M KOH, which was kept in the original plastic bottle as delivered.

**Determination of *K*<sub>a</sub> for the First Deprotonation Step.** A sample of the 1,2-cyclopropanediammonium dibromide (0.250 mmol) was dissolved in water (50.0 mL). The syringe was flushed with 0.100 M KOH from the buret, and the tip of the syringe was placed a few millimeters above the surface of the magnetically stirred solution. KOH (0.100 M, 0.50 mL) was added to the solution, stirring was interrupted, and the pH value was recorded after attaining a constant value, which took 0.2–1 min. Stirring was started again, and a total of 10 portions (0.10–0.15 mL) of 0.100 M KOH was added. After each addition, the pH value was recorded as described.

**Determination of *K*<sub>a</sub> for the Second Deprotonation Step.** KOH (0.100 M, 3.00 mL) was added to water (50.0 mL), followed by a sample of the 1,2-cyclopropanediammonium dibromide (0.250 mmol). The solution was titrated as before. Each compound was titrated twice.

**Calculation of the p*K*<sub>a</sub> Values.** A total of 10 data points from the first deprotonation step and 10 from the second were used for the calculation of the p*K*<sub>a</sub> values with the help of the iterative programme by Albert and Serjeant.<sup>4</sup> The standard deviation of each p*K*<sub>a</sub> value was less than 0.04.

**Equilibrium Constant *K*<sub>T</sub> of the Monocations *trans*-**3b**·H<sup>+</sup>.** Cyclopropanediammonium dibromide *trans*-**3b**·2HBr (152.0 mg, 0.550 mmole) was dissolved in water (10.0 mL) in the apparatus used for the titrations. The pH value was determined (3.989), and the <sup>1</sup>H NMR spectrum was recorded

(29) De Marco, A. *J. Magn. Reson.* **1977**, *26*, 527.



at 25 °C from an aliquot of the solution (500  $\mu$ L). KOH (0.100 M, 0.50 mL) was added from the buret followed by recording of the pH and the  $^1\text{H}$  NMR spectrum at 25 °C. This procedure was repeated seven times. The final pH value was 6.163. For the second deprotonation step, the apparatus was charged with water (10.0 mL) followed by 0.100 M KOH (4.50 mL) and *trans*-**3b**·2HBr (152.0 mg, 0.550 mmol). The procedure described for the first deprotonation step was followed except that three 1-mL portions and, subsequently, three 0.5-mL portions of 0.100 M KOH were added. The initial pH value was 6.295, the final 9.465. The results are shown in Figure 1.

The results shown in Figure 3 were obtained in the same way from *trans*-**1b**·2HBr.

**NOE Experiments with *trans*-**3b**·2HBr.** A solution (0.05 M) of *trans*-**3b**·2HBr (9.66 mg) in  $\text{D}_2\text{O}$  (0.7 mL) was kept at 25 °C in the insert of the 400-MHz NMR spectrometer. The 90° pulse angle was determined<sup>30</sup> with the help of the *N*-methyl singlets.  $T_1$  was estimated.<sup>31</sup> 2-H of the cyclopropane ring showed the longest  $T_1$  (3.3 s). NOE difference spectra were obtained by subtracting 400 spectra recorded with selective saturation (decoupler attenuation 40 dB) of an *N*-methyl group (90° pulse) and 400 spectra recorded with the saturation frequency set outside the interesting area. Complete recovery was achieved by a delay of 30 s after each pulse. A spectrum, recorded with a sweep width of 2.3364 kHz and 16K data points in the time domain, pulse angle = 90°, delay = 30 s, and 8 pulses, afforded the phase correction used for the NOE difference spectra.

Irradiation of the *N*-methyl group absorbing at 2.93 ppm increased the signal of  $\text{H}^2$  (3.27 ppm) and  $\text{H}^3$  (1.44 ppm, *cis* to the *C*-methyl group). Irradiation of the high-field *N*-methyl signal (2.86 ppm) increased the signals of  $\text{H}^2$  and  $\text{H}^4$  (1.76 ppm, *trans* to the *C*-methyl group). The signal of  $\text{H}^2$  showed the largest enhancement in both experiments as expected, because  $\text{H}^2$  is virtually equidistant to both *N*-methyl groups and has the longest relaxation time.

**Kinetic Experiments.** The buffer solutions were kept at

35 °C. An NMR sample tube was charged with buffer solution (500  $\mu$ L), *trans*-**3a**·2HBr (6.21 mg, 0.025 mmol), and sodium 3-(trimethylsilyl)propanesulfonate (1.5 mg). Integration of the signals was impossible because the concentration was too low and the baseline was disturbed by the nearby water signal. This signal also prevented the use of a pulsed NMR spectrometer because it lead to detector overload at high amplification. At low amplification, the signal-to-noise ratio was too bad within the short periods of time (<1 min) required by the fast rates of reaction. Therefore, the NMR spectra were recorded on the CW spectrometer whose insert temperature (35 °C) was determined before and after each experiment. The first spectrum was taken 1.5 min after dissolving of *trans*-**3a**·2HBr in the buffer solutions. Intervals of 10–30 s were maintained between the scans. The heights of the methyl signals of *trans*-**3a**, **8**, and the standard were employed for the calculation of the rate constants. Only the methyl signal of *trans*-**3a** was used for the very fast reactions. The yield of **8**, obtained from *trans*-**3a** in phosphate buffer of pH = 6.8 (95–98%), was determined by cutting and weighting the methyl signals from 5 spectra (0.6 Hz/cm) recorded during the first 5 min and after 5 h at 35 °C.

The pH values were taken with a glass electrode from samples that were identical with those of the NMR experiments.

**Catalysis by Acetone and Butanone.** Acetone (145  $\mu$ L) was added to phosphate buffer solution (pH = 6.8, 0.5 M, 50.0 mL). This solution (50 mM) was further diluted to 2, 3, 4, and 5 mM by adding the appropriate amounts of buffer solution. Solutions of butanone were prepared in the same way.

**Acknowledgment.** We thank Professor Lloyd M. Jackman, The Pennsylvania State University, for many illuminative discussions. Financial support of this work by the Deutsche Forschungsgemeinschaft and the Fonds der Chemischen Industrie, Frankfurt am Main, is gratefully acknowledged.

JO952172Y

(30) Haupt, E. *J. Magn. Reson.* **1982**, *49*, 358.

(31) Martin, M. L.; Delpuech, J. J.; Martin, G. J. *Practical NMR Spectroscopy*; Heyden and Sons: London, 1980; pp 246–275.